W. Washtien, *J. Am. Chem. Soc.*, **96**, 7998 (1974); (e) R. N. F. Thorneley and H. Diebler, *ibid.*, **96**, 1072 (1974).
(13) S. B. Smith and T. C. Bruice, *J. Am. Chem. Soc.*, **97**, 2875 (1975).
(14) T. C. Bruice and Y. Yano, *J. Am. Chem. Soc.*, **97**, 5263 (1975).
(15) (a) K. Koehler, W. Sandstrom, and E. H. Cordes, *J. Am. Chem. Soc.*, **86**, 2413 (1964); (b) N. Gravitz and W. P. Jencks, *ibid.*, **96**, 489 (1974).
(16) R. F. Williams, S. Shinkai, and T. C. Bruice, submitted for publication.
(17) M. J. Gibian and J. A. Rynd, *Biochem. Biophys. Res. Commun.*, **34**, 594 (1969).
(18) R. P. Bell and D. J. Barnes, *Proc. R. Soc. London, Ser. A*, **318**, 421 (1970).
(19) M. L. Ahrens, M. Eigen, W. Kruse, and G. Maass, *Ber. Bunsenges. Phys. Chem.*, **74**, 380 (1970).
(20) F. J. Bullock and O. Jardetsky, *J. Org. Chem.*, **30**, 2056 (1965).
(21) (a) R. P. Bell, "The Proton in Chemistry", 2d ed, Cornell University Press, Ithaca, N.Y., 1973, p 262; (b) *Chem. Soc. Rev.*, **3**, 513 (1974).
(22) J. E. Dixon and T. C. Bruice, *J. Am. Chem. Soc.*, **92**, 905 (1970).
(23) (a) B. G. Barman and G. Tollin, *Biochemistry*, **11**, 4760 (1972); (b) J. H. Swinehart, *J. Am. Chem. Soc.*, **87**, 904 (1965).
(24) R. W. Taft, "Proton Transfer Reactions", E. F. Caldin and V. Gold, Ed., Chapman and Hall, London, 1975, p 64.
(25) T. C. Bruice, *Prog. Bioorg. Chem.*, in press; R. F. Williams, S. Shinkai, and T. C. Bruice, *Proc. Natl. Acad. Sci. U.S.A.*, **72**, 1763 (1975).

Conformational Interconversions of *cis,cis*-Cyclooctadiene-1,5

Otto Ermer

Contribution from the Abteilung für Chemie, Ruhr-Universität, D 463 Bochum, West Germany. *Received September 9, 1975*

Abstract: A detailed force-field study of conformational changes of *cis,cis*-cyclooctadiene-1,5 (I) is presented. A number of methodical points concerning the calculation of transition states and potential energy profiles are mentioned. All energy minimizations were performed by efficient and accurate Newton–Raphson techniques. Three potential energy minima and four transition states were found relevant for a description of the conformational properties of I. The transition states are characterized by their "transition coordinate"; i.e., by the eigenvector of the negative eigenvalue of the mass-weighted matrix of second derivatives of the potential energy. The seven calculated conformations are essentially characterized by different distributions of angle and torsional strain; the differences of the other strain factors are less pronounced. A complete set of thermodynamic properties was calculated. The most favorable calculated conformation of I is a twist-boat structure of symmetry C_2 (C–CH_2–CH_2–C torsion angles 52.5°), in agreement with experimental evidence. Potential energy profiles for three different twist-boat/twist-boat interconversion processes were evaluated. The process via a twist transition state of D_2 symmetry has the lowest calculated free enthalpy of activation ($\Delta G^{\ddagger}$ = 4.15 kcal mol^{-1} at 100 K) and is suggested to interpret a ^{1}H NMR coalescence of I observed at 96 K ($\Delta G^{\ddagger}$ = 4.4 ± 0.1 kcal mol^{-1}) by Anet and Kozerski.[1] The other two processes [via a boat transition state (C_{2v} symmetry) and an intermediate chair minimum (C_{2h} symmetry), respectively] have calculated $\Delta G^{\ddagger}$ values (at 100 K) of 5.73 and 5.91 kcal mol^{-1}. Both the chair process and a combination of twist and boat processes are offered to explain a second observed ^{1}H NMR coalescence at 105 K[1] ($\Delta G^{\ddagger}$ = 4.9 ± 0.1 kcal mol^{-1}).

Conformational changes of *cis,cis*-cyclooctadiene-1,5 (I) have recently been studied experimentally by Anet and Kozerski[1] (low-temperature NMR measurements) and computationally by Allinger and Sprague[2] (force-field calculations). We wish to report the results of another force-field study which are well compatible with the results and interpretations of Anet and Kozerski but less so with Allinger's and Sprague's calculations.

Method

The method of calculation has been outlined in a recent publication.[3] The consistent force field used has also been described earlier.[4] Some further methodical points of interest are mentioned below where appropriate.

Results

Altogether seven conformations were found important for a description of the conformational properties of I. Three correspond to potential energy minima (M_1, M_2, M_3), four to one-dimensional partial maxima (saddle points, transition states: T_1, T_2, T_3, T_4). By applying Newton–Raphson iterations to suitable starting geometries, the internal parameters of Figure 1 were obtained. The final average absolute derivatives of the potential energy V with respect to the Cartesian atomic coordinates were in all cases less than 10^{-6} kcal mol^{-1} Å^{-1}. Vibrational frequencies and principal moments of inertia were calculated and used for the evaluation of the thermodynamic properties of Table I. Calculated potential energy paths relating the minima and transition states of Figure 1 are given in Figures 2–4.

Discussion

Potential Energy Minima. The available experimental evidence indicates that the most favorable conformation of I in the gas phase[5] and in solution[1] is the twist-boat form of symmetry C_2 (M_1, Figure 1), in agreement with Allinger's and Sprague's and our calculations. This conformation was also observed in the crystals of two derivatives of I, namely, *syn*-3,7-dibromo-*cis,cis*-cyclooctadiene-1,5 (II)[6] and (*all-ax*)-4,8-dimethyl-*cis,cis*-cyclooctadiene-1,5-dicarboxamide-3,7 (III).[7] The ring geometries observed in these two crystals are also given in Figure 1. It appears that in both cases the eight-ring boats are more twisted than calculated for I [C–CH_2–CH_2–C torsion angles observed for II and III are 65 and 76° (average), respectively (Figure 1); calculated 52.5° (Figure 1); calculated by Allinger and Sprague, 37.9° [2]]. To what degree this difference reflects the various intra- and intermolecular perturbations exerted on the conformation of the eight-membered ring by the substituents (and the other packing forces) in the crystals of II and III cannot be decided from the results of the calculations presented here. It can be said, however, that the energy difference of the eight-ring conformations in the crystals of II and III, and our calculated geometry is rather small (see below). M_1 is characterized by a low torsional energy yet appreciable angle strain (Table I) which originates from a transannular H···H repulsion (Figure 1; corresponding calculated H···H distance, 1.992 Å). Another manifestation of this interaction is an abnormally high calculated symmetric CH_2-scissoring frequency (A-mode) of 1560 cm^{-1}. MacNicol et al.[6] interpret an observed band of solid II at 1487 cm^{-1} as this unusual scissoring vibration.

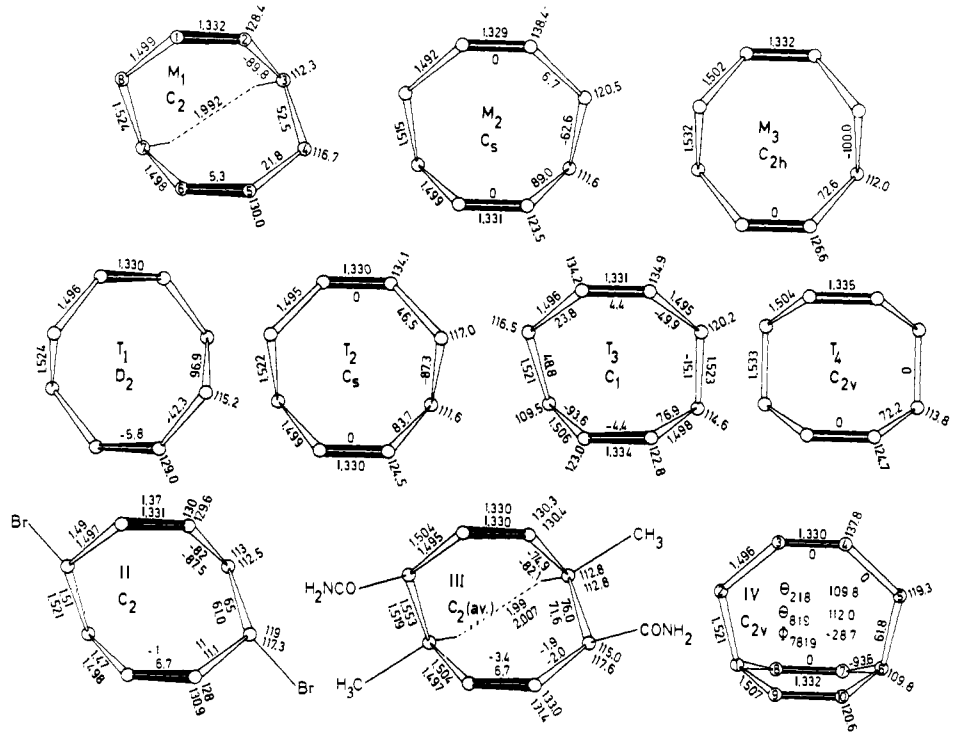

Figure 1. Top seven diagrams: calculated geometry parameters of *cis,cis*-cyclooctadiene-1,5 conformations (M_1, M_2, M_3 potential energy minima; T_1, T_2, T_3, T_4 one-dimensional partial maxima = transition states). Two lower left diagrams: experimental geometries (C_2 averages in case of III; the eight-ring geometry observed in the crystals of III does not significantly differ from C_2 symmetry[7]) in the crystals of two cyclooctadiene derivatives (top values) and calculated values obtained by mapping. Lower right diagram: calculated geometry of bicyclo[4.2.2]decatriene-3,7,9. Peripheral values, bond lengths and angles (Å, deg); others, torsion angles (deg).

Table I. Calculated Strain Contributions and Thermodynamic Properties of *cis,cis*-Cyclooctadiene-1,5 Conformations[a,c]

	M_1[b]	M_2	M_3	T_1	T_2	T_3	T_4
Symmetry	C_2	C_s	C_{2h}	D_2	C_s	C_1	C_{2v}
ΔV_l[d]	*0.03*	0.13	0.00	0.04	0.02	0.03	0.03
ΔV_θ[d]	*5.51*	7.09	−3.64	0.19	1.63	2.58	−4.20
ΔV_Φ[d]	*5.00*	−2.20	7.88	5.88	4.08	3.43	9.58
ΔV_χ[d]	*0.02*	0.09	0.07	0.01	0.16	0.22	0.09
ΔV_{cross}[d]	*−0.54*	−0.74	0.38	−0.28	−0.24	−0.10	0.70
ΔV_{nbi}[d]	*3.41*	−0.31	−0.60	−0.78	−0.60	0.40	0.88
ΔV	*13.43*	4.07	4.09	5.05	5.06	6.55	7.09
ΔH_{100}[f]	*123.69*	4.40	2.83	3.92	4.25	5.96	5.51
ΔH_{298}	*127.54*	4.38	3.09	3.79	4.03	5.71	5.39
$\Delta S_{vibr,100}$[f]	*2.42*	0.22	0.47	−1.00	−1.09	−0.84	−0.67
$\Delta S_{vibr,298}$	*15.26*	0.17	1.94	−1.71	−2.26	−2.24	−1.31
ΔS_{rot}	*23.33* (100 K) *26.59* (298 K)	1.46	0.06	−1.34	1.48	1.37	−0.12
ΔS_{mix}	*1.38*	−1.38	−1.38	0	−1.38	0	−1.38
ΔS_{100}	*67.07*	0.30	−0.85	−2.34	−0.99	0.53	−2.17
ΔS_{298}	*83.16*	0.25	0.62	−3.05	−2.16	−0.87	−2.81
ΔG_{100}	*116.98*	4.37	2.92	4.15	4.35	5.91	5.73
ΔG_{298}	*102.74*	4.31	2.91	4.70	4.67	5.97	6.23
$-\sqrt{-1}\omega^{\ddagger}$[e]				78.2	91.9	162.2	166.2

[a] For geometry parameters, see Figure 1. [b] The values for M_1 are absolute (given in italics); those of the other conformations are relative to M_1. [c] Units: energy quantities in kcal mol^{-1}, entropies in cal mol^{-1} deg^{-1}, values for $-\sqrt{-1}\,\omega^{\ddagger}$ in cm^{-1}. [d] The symbols l, θ, Φ, χ, cross, and nbi refer to the contributions to the potential energy V of lengths, angles, torsions, out-of-plane bendings at double-bond C atoms,[4] valence force-field cross terms,[4] and nonbonded interactions. [e] $\omega^{\ddagger}$ is the imaginary frequency of the transition states. The other symbols are standard. [f] The enthalpies H and entropies S result from the following relationships: $H = V + H_{vibr} + 3RT = V + \Sigma_{n=1}{}^{D} 0.002858\omega_n \{\frac{1}{2} + [\exp(1.4387\,\omega_n/T) - 1]^{-1}\} + 3RT$; $S = S_{trans} + S_{rot} + S_{vibr} + S_{mix}$ with $S_{trans} = 25.987 + 6.861 \log M$, $S_{rot} = 2.287\,(3 \log T - 2 \log \sigma + \log I_1 I_2 I_3) + 267.55$, $S_{vibr} = 1.9865\,\Sigma_{n=1}{}^{D}\{1.4387\,\omega_n/T[\exp(1.4387\,\omega_n/T) - 1]^{-1} - \ln[1 - \exp(-1.4387\,\omega_n/T)]\}$, $S_{mix} = 1.3769$ for chiral conformations (M_1, T_1, T_3) and zero for nonchiral conformations (ω_n, frequencies in cm^{-1}; M, molecular weight in g mol^{-1}; σ, symmetry number; I_1, I_2, I_3, principal moments of inertia in g cm^2; D, number of real nonzero frequencies, i.e., $3N - 6$ for minima and $3N - 7$ for transition states; N, number of atoms).

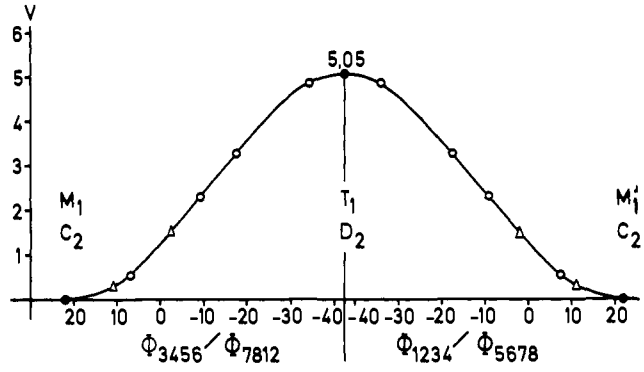

Figure 2. Calculated potential energy profile for the twist process: V, potential energy (kcal mol^{-1}); Φ, mapping parameters (deg). The change of the mapping parameters is indicated by a vertical line at the abscissa. Mapping points are given as open circles (○), minima and transition state as full circles (●) together with potential energies relative to M_1. The triangles represent mapping points which correspond to experimental C-C-C=C torsion angles of derivatives of I (two lower left diagrams of Figure 1). A graphical description of the interconversion and the atom numbering is given in Figure 5.

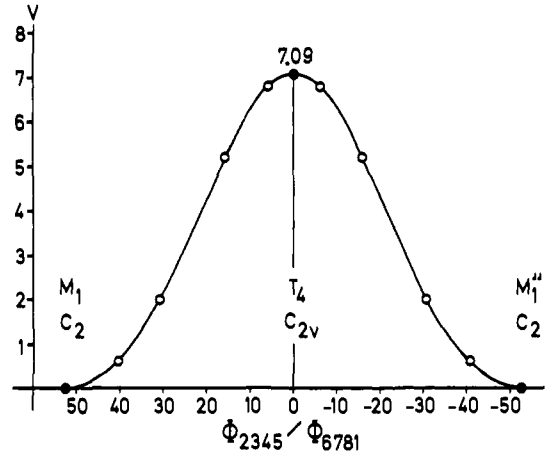

Figure 3. Calculated potential energy profile for the boat process; see legend of Figure 2 for further explanations and Figure 6 for a graphical description of the interconversion and the atom numbering.

The C_{2h} symmetric chair form (M_3) corresponds to a true minimum with a calculated potential energy V higher than that of M_1 by 4.09 kcal mol^{-1} (Table I; ΔH = 3.09, ΔG = 2.91 kcal mol^{-1} at room temperature; ΔV calculated by Allinger and Sprague,[2] 1.45 kcal mol^{-1}). The energy increase is due to the unfavorable torsion angles of M_3 as compared with M_1 around both types of CC single bonds (Figure 1, Table I). In the dibenzo compound this energetical disadvantage is very probably less pronounced since here the rotational barrier around the C(sp3)-C(sp2) bonds is expected to be smaller than in the parent compound I[2,4] as a consequence of its similarity to the sixfold methyl rotation barrier in toluene. (An energy minimization of M_1 and M_3 with this barrier set to zero in our force field yields a potential energy for M_3 only 0.19 kcal mol^{-1} higher than for M_1 and C-CH_2-CH_2-C torsion angles of 39.2° for M_1; Allinger and Sprague calculated a difference of 1.30 kcal mol^{-1} for the dibenzo compound in favor of the twist-boat and 26.5° for the torsion angles mentioned.) Accordingly, there are crystallographic indications that in the crystals of the dibenzo compound, the eight-membered ring has the centrosymmetric chair conformation since the space group of these crystals has been found to be $P2_1/c$ with two molecules in the unit cell.[8] Because of bad own experiences with such arguments, we wish to remark that this reasoning is of course not completely conclusive since it presupposes an

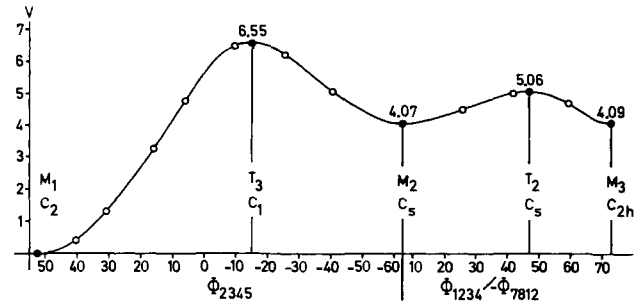

Figure 4. Calculated potential energy profile for the chair process. For a complete profile of a twist-boat/twist-boat interconversion, the diagram has to be continued at M_3 by its mirror image. See legend of Figure 2 for further explanations and Figures 7 and 8 for a graphical description of the interconversion and the atom numbering.

ordered crystal structure. (In the course of crystallographic studies of cyclodecane-1,6-diols we had to accept that certain crystals with space group $P2_1/c$ and six molecules in the unit cell contained only cis diol molecules and hence were not ordered. Before the detailed structure analysis we had concluded that at least two diol molecules in the unit cell were trans configurated and therefore capable to adopt a centrosymmetric geometry in these crystals.[9]) Thus, before definite conclusions, the results of a complete crystal structure analysis of the dibenzo compound have to be awaited. We are presently performing this analysis.

The C_s symmetric conformation M_2 (Figure 1) corresponds to a true potential energy minimum and has almost the same calculated potential energy as the chair M_3. It forms an intermediate species of our calculated twist-boat/chair interconversion path (see below). Allinger and Sprague[2] discuss a conformation apparently similar to M_2 as a transition state. M_2 has very favorable torsion angles; the respective energetic advantage is, however, outweighed by a very high angle strain (Figure 1, Table I): two C-C=C angles are opened out to 138.4°. (This result obviously contains some degree of uncertainty since we work with harmonic angle bending functions,[4] the transferability of which to angle deformations of this magnitude has not been established: experimentally.)

A conformation similar to M_2 is discussed below as a calculated conformational element of a bicyclodecatriene system.

Transition States and Interconversion Paths. The twist-boat conformation M_1 contains four symmetry independent methylene protons. Three energetically different processes are conceivable which lead to time-averaged eight-ring structures with two and one independent CH_2 protons, i.e., with two groups of four equivalent and eight equivalent CH_2 protons, respectively. The corresponding time-averaged symmetries of I are D_2, C_{2v}, and D_{2h} for twist-boat/twist-boat interconversions across the transition states T_1 (twist form, D_2 symmetry) and T_4 (boat, C_{2v}) and via the minimum M_3 (chair, C_{2h}), respectively (Figure 1, Table I). In the following we discuss some details of these processes.

Twist Process (time-averaged symmetry of I, D_2; i.e., two groups of four equivalent CH_2 protons). A calculated potential energy path for this interconversion is shown in Figure 2. The D_2 symmetric transition state T_1 was calculated by applying steepest-descent and Newton-Raphson iterations to a suitable trial structure of exact D_2 symmetry, utilizing the phenomenon of symmetry conservation.[3] The fact that the F matrix ($F_{ij} = \partial^2 V/\partial x_i \partial x_j$; x_i, Cartesian atomic coordinates) of the optimal geometry of T_1 was found to contain one negative eigenvalue simultaneously proved T_1 to be a transition state (one-dimensional partial maximum). The mapping points given in Figure 2 (as well as those of the profile of the following process) were mainly calculated in order to establish the absence of intermediate minima and maxima on going from M_1 to T_1. The

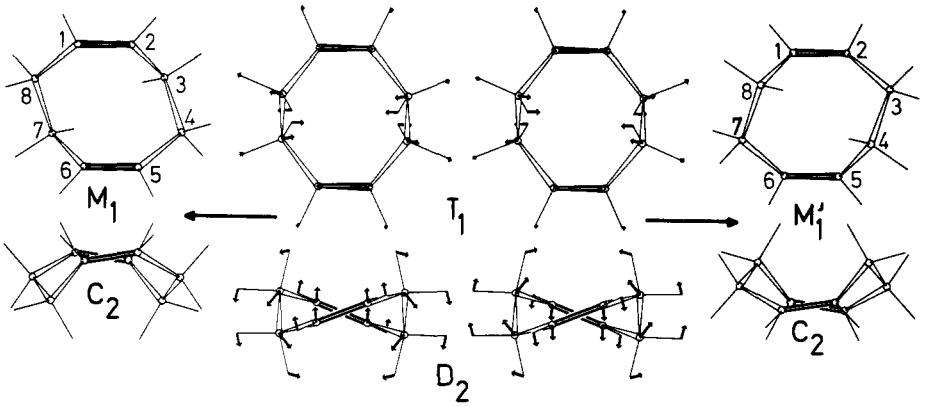

Figure 5. Graphical representation of the twist process. The displacements of the transition coordinate are mass weighted (see text for details).

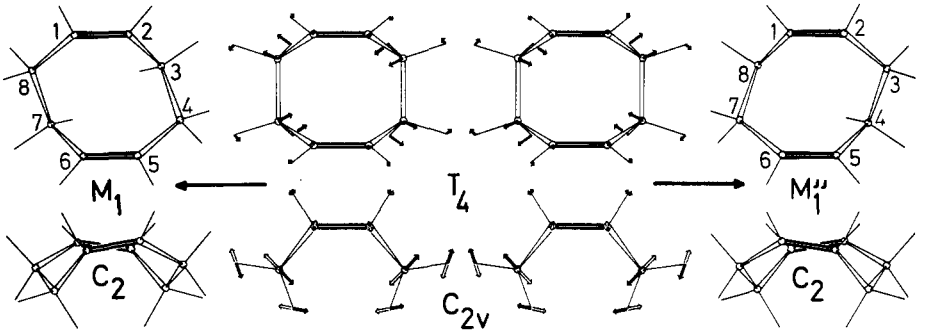

Figure 6. Graphical representation of the boat process. The atomic displacements of the obscured rear atoms in the side views of the transition coordinate of T_4 are given as open arrows (see legend of Figure 5).

changes of the torsion angles forming the abscissa of Figure 2 do not completely describe the reaction path. They only represent characteristic and large components of this path; i.e., these changes are only an incomplete model of the reaction path. We therefore do not use the term "reaction coordinate" for these torsion angles as is often done but rather apply the term "mapping parameters". Not considering kinetic energy effects, the path of a reaction is that of steepest potential energy descent on going from the transition state to the minimum. The reaction path at a particular molecular geometry formed during the reaction is thus completely described by a vector, the components of which are relative atomic displacement coordinates that define the direction of the steepest descent path at this point. At the transition state this vector is given in a straightforward way as the eigenvector belonging to the one negative eigenvalue of the $\boldsymbol{F}$ matrix associated with the transition state. This vector was originally called "Talverbindungslinie" by Pelzer and Wigner[10] in a classical paper on transition-state theory. At the transition state, we consider in the present paper also the influence of the kinetic energy and characterize a transition state by the corresponding eigenvector of the *mass-weighted* $\boldsymbol{F}$ matrix ($\boldsymbol{M}^{-1/2}\,\boldsymbol{F}\boldsymbol{M}^{-1/2}$; $\boldsymbol{M}$ diagonal matrix with diag($\boldsymbol{M}$) = $m_1, m_1, m_1, m_2, m_2, m_2, m_3, \ldots, m_N, m_N, m_N$; N number of atoms) which gives a picture of the actual *motions* of the atoms when crossing the transition state barrier along the minimum energy path. We call this eigenvector the *transition coordinate;* it is the normal coordinate—expressed in mass-weighted Cartesian coordinates—of the imaginary frequency (square root of the negative eigenvalue of the mass-weighted $\boldsymbol{F}$ matrix) belonging to the transition state. The imaginary frequencies of the calculated transition states appear in Table I.

In Figures 5-8 graphical descriptions of the four calculated conformational transitions of I are presented. The interesting parts of the diagrams are the transition coordinates given as quadruplets of vector sets (top and side views). The phases of the atomic displacements of the left and right transition coordinate diagrams of a transition state are opposite, leading to the left and right minimum, respectively. (The scale of the sets of displacement amplitudes is arbitrary; within one transition coordinate, the amplitudes are relative quantities. Apart from this arbitrariness, the diagrams are drawn to scale. The displacements of the diagrams are mass weighted; division of these displacements by the square root of the appropriate atomic masses leads to the actual undistorted displacements.) The transition coordinate diagrams give a good representation of the symmetry properties and the dynamic nature of the transition states, just in the same way as usual normal coordinates describe the symmetries and the dynamics of real vibrations. They also can serve to illustrate how one has to distort molecular geometries corresponding to partial energy maxima if, during a search for true minima, one wants to get rid of partial maxima. (It is better for this purpose, however, to use the eigenvectors of the negative eigenvalues of $\boldsymbol{F}$ itself which do not include kinetic energy effects, as has been done by McIver and Komornicki[11] in the course of quantum-mechanical calculations of transition states. In general, for heteronuclear systems the mass scaling severely affects the relative magnitudes of the atomic displacements. It also leads to different directions of the displacements, although not very pronounced in case of our mainly torsional transition coordinates. In special cases the directions of the displacements are not changed by mass scaling, e.g., for out-of-plane deformations of planar molecules, or an eigenvector is completely unchanged, e.g., for the twisting deformation of ethylene.)

The mapping points connecting M_1 and T_1 in Figure 2 were calculated with the constraint that the twofold axis not passing through bond centers was preserved. A necessary condition for performing such symmetry-constrained mappings is that the transition coordinate corresponds to a mode which is symmetric with respect to the symmetry element(s) which is (are) preserved. For T_1 the transition coordinate corresponds to a

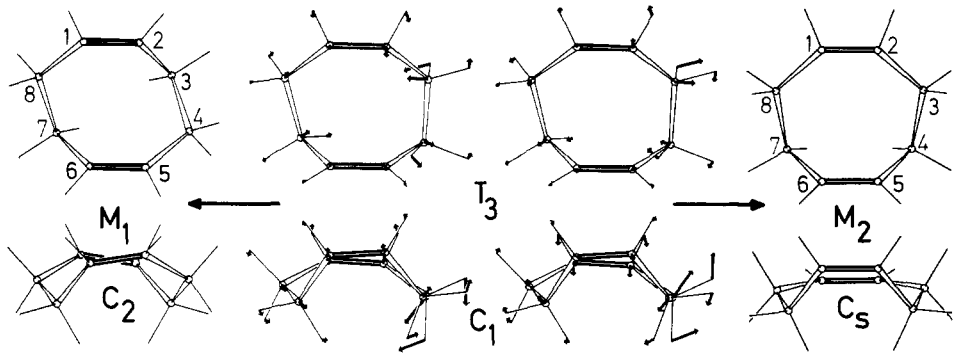

Figure 7. Graphical representation of the M_1/M_2 interconversion (first step of the chair process); see legend of Figure 5.

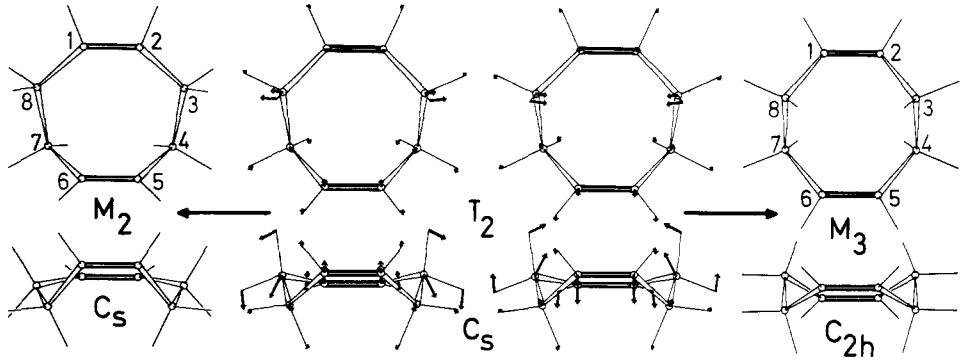

Figure 8. Graphical representation of the M_2/M_3 interconversion (second step of the chair process); see legend of Figure 5.

B mode being symmetric with respect to the twofold axis not passing through bond centers (Figure 5). In the present case the symmetry constraint was introduced by adding to the derivatives of V the contributions of the same constraint potentials $K_c(\Phi - \Phi_c)^2$ for *two* C-C-C=C torsion angles related by the twofold axis in question (Figure 2; K_c, large fictitious torsional potential constant; Φ, mapped torsion angle; Φ_c, mapping value; see ref 3 for methodical details). The derivatives of V modified by the contributions of the two constraint potentials still contain the desired twofold symmetry which cannot get lost in the course of the constrained minimizations.[3] The energy profile of Figure 2 is a composite diagram as explained below.

The calculated activation parameters $\Delta V^{\ddagger}$, $\Delta H^{\ddagger}$, $\Delta G^{\ddagger}$, and $\Delta S^{\ddagger}$ for the twist process are 5.05, 3.92, 4.15 kcal mol^{-1} and -2.34 cal mol^{-1} deg^{-1}, respectively (Table I; calculated at 100 K for below comparison with the measurements of Anet and Kozerski[1]; room-temperature values are also contained in Table I). $\Delta V^{\ddagger}$ is mainly a torsional energy difference (Table I, Figure 1).

The observed geometries of the eight-membered rings in the crystals of II and III are similar to calculated geometries corresponding to points on the profile of Figure 2 with the experimental torsion angles taken as mapping values. [These two points are indicated in Figure 2; as mentioned above, the energy increase relative to M_1 is rather small. Calculated geometry parameters at both points are reproduced in Figure 1; the overall fit of these geometries with those observed for II and III could have been further improved by taking mapping parameter values somewhat smaller than the respective observed torsion angles. The rather large difference of the C—C=C—C torsion angles (Figure 1) would remain, however. The origin of this difference is not clear; in the calculations the slight nonplanar deformation of the double bonds helps to improve the adjacent C—C—C=C torsion angles.] Paths of reactions involving the formation or breaking of bonds have recently been correlated with crystal structural data by Bürgi, Dunitz et al.[12] It appears feasible that their ideas can also be applied to the study of conformational interconversion paths. This would mean that conformational perturbations caused by substituents and/or crystal forces prefer to follow a conformational interconversion path of the parent gaseous compound as suggested by the above example.[13] Another example is discussed in connection with the following process.

Boat Process (time-averaged symmetry of I, C_{2v}; i.e., two groups of four equivalent CH_2 protons). A calculated potential energy profile for this interconversion is shown in Figure 3. The C_{2v}-symmetric transition state T_4 was calculated in the same way as the D_2-symmetric transition state T_1 by making use of the additional symmetry elements as compared with M_1. The mapping points of Figure 3 were again calculated such that the twofold axis of symmetry was preserved, and the two C-CH_2-CH_2-C torsion angles were taken as mapping parameters. The transition coordinate of T_4 corresponds to a A_2 mode which is symmetric with respect to the twofold axis and antisymmetric with respect to the two mirror planes (Figure 6), thus justifying the symmetry-constrained mapping.

The calculated activation parameters $\Delta V^{\ddagger}$, $\Delta H^{\ddagger}$, $\Delta G^{\ddagger}$, and $\Delta S^{\ddagger}$ for the boat process are at 100 K 7.09, 5.51, 5.73 kcal mol^{-1}, and -2.17 cal mol^{-1} deg^{-1}, respectively (Table I). Compared with M_1 the transition state T_4 has a very unfavorable torsional energy, yet less angle strain (Table I, Figure 1). An alternative route for the boat process with different strain characteristics is discussed below.

The crystal structures of a number of metal complexes containing I as a chelate ligand have been analyzed,[14] and twist-boat conformations were found which are less twisted than our calculated geometry for I because the boat conformation is more favorable for complex formation. The detailed eight-ring geometries in the complexes closely resemble calculated geometries corresponding to mapping points of Figure 3, in a similar way as discussed above for the derivatives II and III with observed eight-ring structures more twisted than calculated. In the crystals of *cyclo*-di-β-alanyl relatively

slightly twisted eight-membered rings of C_2 symmetry were also observed[15] ($C-CH_2-CH_2-N$ torsion angles 27°), although we have recently found remarkable conformational similarities between calculated cycloolefin conformations[4] and experimental conformations of the corresponding lactams.[16] The origin of the discrepancies for *cyclo*-di-β-alanyl is not simply evident.

In bicyclo[4.2.2]decatriene-3,7,9 (IV)[17] the two cyclooc-

IV

tadiene systems are calculated to have a conformation very similar to M_2. IV has calculated C_{2v} symmetry such that the two equivalent eight-membered rings have six consecutive coplanar carbon atoms in common. The M_2-like conformations in IV are a consequence of the fact that this geometry is the only possibility for *both* eight-membered rings to avoid an unfavorable boat-like conformation (see also the following discussion of the chair process). This energetic compromise (at the expense of angle strain) does, however, not lead to a very rigid structure: The calculated potential of IV is fairly shallow with respect to deformations perpendicular to the plane containing the six carbon atoms mentioned; the calculated lowest frequency for a deformation of this type (a B-mode symmetric with respect to the mirror plane bisecting the three double bonds) amounts to 115.4 cm^{-1}. Calculated internal parameters of IV are included in Figure 1. We are currently investigating the crystal structure of a derivative of IV.

Chair Process (time-averaged symmetry of I, D_{2h}; i.e., all CH_2 protons equivalent; a complete averaging of these protons is also effected by a combination of the twist and boat processes). A potential energy profile of this process which proceeds via the C_{2h} symmetric chair M_3 is given in Figure 4. The chair process is more complex than the two processes already discussed; it leads via the intermediate minimum M_2 without conservation of the twofold axis of M_1. The transition state T_3 between M_1 and M_2 possesses no symmetry, and as a mapping parameter *one* $C-CH_2-CH_2-C$ torsion angle was used (Figures 4 and 7). In the course of this mapping, the second $C-CH_2-CH_2-C$ torsion angle does not change very much and keeps its favorable value. The corresponding smaller increase of the torsional energy on going to T_3 (as compared with the boat process) is, however, largely compensated by more angle strain. T_3 was calculated by applying Newton-Raphson iterations to a suitable adjacent geometry obtained by the mapping just mentioned (Figures 4 and 7; see ref 3 for methodical details).

From M_2 the chair conformation M_3 is reached via a shallow, second, one-dimensional partial maximum (T_2) which has C_s symmetry. T_2 already has the shape of a chair conformation. (This is also true for M_2, although much less pronounced; cf. the torsion angles given in Figure 1.) Like T_3, it cannot be calculated making use of its symmetry since the adjacent minimum M_2 has the same symmetry as T_2, while M_3 contains additional symmetry elements as compared with T_2. Thus partial mapping for roughly locating T_2 could again not be avoided.[3] The mapping was performed by constraining two C—C—C=C torsion angles related by the mirror plane to values of opposite sign and equal magnitude, thus preserving this symmetry element (Figure 4). [The transition coordinate of T_2 has the appropriate symmetry, i.e., it is symmetric with respect to the mirror plane (Figure 8).] We do not discuss T_2 further since it is not a rate-determining barrier.

Dunitz and Waser have shown by analytical geometric reasoning[18] that the C_{2h} symmetric chair conformation of I with fixed CC lengths and CCC angles is rigid, just in the same way as the cyclohexane chair conformation with fixed lengths and angles. They have also pointed out that from this analytical result (which essentially reflects properties of Dreiding models), no conclusions can be drawn as to the *degree* of rigidity in both systems. This is only possible by involving physical principles as, for example, in the present calculations. From these, the chair conformation of I results much less rigid than the cyclohexane chair as we have described in the preceding paragraph. The reason for this is that the cyclohexane chair has almost optimal angles *and* torsion angles, whereas the chair of I has a high torsional strain which can be transformed into angle strain with little change of the total potential energy.

We want to emphasize that in our calculations the C_{2v} symmetric transition state T_4 (boat) is not a transition state for the twist-boat/chair interconversion as has been discussed by other authors.[1,2] This is clearly evident from the symmetry of the transition coordinate of T_4 which, as mentioned, is antisymmetric with respect to the mirror plane bisecting the double bonds (Figure 6). An interconversion of T_4 to M_2 and subsequently to the chair M_3 (via T_2) leads across a two-dimensional partial maximum (i.e., not along a feasible path[11]) of C_s symmetry with a potential energy 0.43 kcal mol^{-1} above T_4 and imaginary frequencies of 109.1 and 151.1$\sqrt{-1}$ cm^{-1}.

The continuation of the $M_1-T_3-M_2$ profile by its mirror image yields an alternative interconversion path for the boat process. A path of this kind avoids the simultaneous passing of the two $C-CH_2-CH_2-C$ torsion angles through zero, as mentioned above; this path for the boat process would be hidden in the twist-boat/chair interconversion since T_3 is the rate-determining barrier also for the chair process which leads to the equivalence of all methylene protons.

The profile given in Figure 4 for the chair process is a composite diagram consisting of two different consecutive simple transitions evaluated with different mapping parameters. It is clear that, in general, for a composite profile the mapping parameters can only be changed at minima or transition states where the profile has zero slope and a smooth connection between the partial diagrams is ensured. (The profile of the twist process as given in Figure 2 is also a composite diagram with a change of the mapping parameters at the transition state. The mapping could have been performed without this change but this would lead to an asymmetric profile with more mapping points to calculate. Because of the symmetry of T_1, the change of the mapping parameters leads to two symmetry equivalent halves of the diagram, of which only one has to be mapped. The $C-CH_2-CH_2-C$ torsion angles are not suitable mapping parameters for the twist process since they do not change in one sense during the transition but rather pass through an extremal value.) Mapping parameters should be selected in such a way that they change drastically in one sense (only increasing or only decreasing) during the transition they are intended to describe.

The calculated activation parameters for the rate-determining step of the chair process are at 100 K 6.55, 5.96, 5.91 kcal mol^{-1} for $\Delta V^{\ddagger}$, $\Delta H^{\ddagger}$, $\Delta G^{\ddagger}$ and 0.53 cal mol^{-1} deg^{-1} for $\Delta S^{\ddagger}$. The origin of $\Delta V^{\ddagger}$ has been characterized above.

Conclusions

Summarizing our discussion of the three calculated potential energy minima and the four transition states of I, we note that all seven conformations are mainly characterized by different distributions of angle and torsional strain (Table I); the differences of the other strain factors are less distinct yet not negligible: The maximum differences of the cross-term contributions and the nonbonded interactions each amount to about 1.5 kcal mol^{-1}.

Anet and Kozerski have observed by low-temperature NMR techniques two absorption coalescences (^1H NMR spectra of

l in solution) corresponding to $\Delta G^{\ddagger}$ values of 4.4 ± 0.1 (at 96 K) and 4.9 ± 0.1 kcal mol^{-1} (at 105 K).[1] They interpreted these as originating from twist-boat/twist-boat interconversion processes and concluded that the coalescence at lower temperature is due to either the twist or the boat process, the one at higher temperature either to the combined twist and boat processes or to the chair process. In principle, it can be decided from the study of suitably deuterated species of I (e.g., V) what

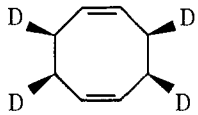

V

the nature of the low-temperature coalescence is,[1] but it is not possible to decide experimentally whether the high-temperature coalescence originates from the chair process or from a combination of the twist and boat processes. Our results (Table I) suggest that the low-temperature coalescence is caused by the twist process (calculated $\Delta G^{\ddagger}_{100}$ = 4.15 kcal mol^{-1}), while for the high-temperature coalescence both the combined twist and boat processes [calculated $\Delta G^{\ddagger}_{100}$ (for boat process) = 5.73 kcal mol^{-1}] and the chair process (calculated $\Delta G^{\ddagger}_{100}$ = 5.91 kcal mol^{-1}) have to be taken into consideration. Allinger and Sprague favor the boat process for explaining the low-temperature coalescence.[2]

We want to conclude our discussion with a comment on terminology. Conformational interconversions of the kind described here are often referred to as proceeding along pseudorotational paths despite the fact that substantial energy barriers of several kilocalories have to be overcome. We wish to advocate that the term pseudorotation should be reserved for cyclic interconversion processes with no barrier (or at most with barriers *very* close to zero), i.e., with a constant potential along the interconversion path, as originally intended by Pitzer et al.[19] Cyclic interconversions with barriers similar to those discussed here should rather be termed *hindered* pseudorotational processes.[20]

Acknowledgment. Financial support of the Deutsche Forschungsgemeinschaft is gratefully acknowledged.

References and Notes

(1) F. A. L. Anet and L. Kozerski, *J. Am. Chem. Soc.*, **95**, 3407 (1973). NOTE ADDED IN PROOF: For a short account of recent conformational calculations on I by these authors, see F. A. L. Anet and R. Anet in "Dynamic Nuclear Magnetic Resonance Spectroscopy", F. A. Cotton and L. M. Jackman, Ed., Academic Press, New York, N.Y., 1975, p 571. We thank Dr. Anet, a referee of this paper for pointing out this reference, and for informing us that "on the whole" their results agree with ours.
(2) N. L. Allinger and J. T. Sprague, *Tetrahedron*, **31**, 21 (1975). The discrepancies between Allinger's and Sprague's and our results are probably mainly due to the fact that the H···H nonbonded function of the former authors is too strongly repulsive, as has also been observed by others: T. Clark, T. McO. Knox, H. Mackle, and M. A. McKervey, *Chem. Commun.*, 666 (1975); D. N. J. White, private communication.
(3) O. Ermer, *Tetrahedron*, **31**, 1849 (1975).
(4) O. Ermer and S. Lifson, *J. Am. Chem. Soc.*, **95**, 4121 (1973).
(5) L. Hedberg and K. Hedberg, see *Perspect. Struct. Chem.*, **4**, 60 (1971).
(6) R. K. Mackenzie, D. D. MacNicol, H. H. Mills, R. A. Raphael, F. B. Wilson, and J. A. Zabkiewicz, *J. Chem. Soc., Perkin Trans. 2*, 1632 (1972).
(7) L. Leiserowitz, private communication; we thank Dr. Leiserowitz for kindly making available his unpublished structural results which appear in Figure 1; see also B. S. Green, M. Lahav, and G. M. J. Schmidt, *J. Chem. Soc. B*, 1552 (1971).
(8) W. Baker, R. Banks, D. R. Lyon, and F. G. Mann, *J. Chem. Soc.*, 27 (1945).
(9) O. Ermer and J. D. Dunitz, unpublished results.
(10) H. Pelzer and E. Wigner, *Z. Phys. Chem., Abt. B*, **15**, 445 (1932).
(11) J. W. McIver and A. Komornicki, *J. Am. Chem. Soc.*, **94**, 2625 (1972). NOTE ADDED IN PROOF: R. E. Stanton and J. W. McIver, *J. Am. Chem. Soc.*, **97**, 3632 (1975), have recently applied symmetry considerations to the characterization of transition states in the course of quantum-chemical calculations.
(12) H. B. Bürgi, *Inorg. Chem.*, **12**, 2321 (1973); H. B. Bürgi, J. D. Dunitz, and E. Shefter, *J. Am. Chem. Soc.*, **95**, 5065 (1973); H. B. Bürgi, J. D. Dunitz, J. M. Lehn, and G. Wipff, *Tetrahedron*, **30**, 1563 (1974).
(13) H. B. Bürgi, *Angew. Chem., Int. Ed. Engl.*, **14**, 460 (1975), and C. Altona, H. J. Geise, and C. Romers, *Tetrahedron*, **24**, 13 (1968), have analyzed the pseudorotational path of cyclopentane in this way.
(14) J. A. Ibers and R. G. Snyder, *Acta Crystallogr.*, **15**, 923 (1962); W. C. Baird and J. H. van den Hende, *J. Am. Chem. Soc.*, **85**, 1009 (1963); M. D. Glick and L. F. Dahl, *J. Organomet. Chem.*, **3**, 200 (1965); H. Dierks and H. Dietrich, *Z. Kristallogr., Kristallgeom. Kristallphys., Kristallchem.*, **122**, 1 (1965); J. Coetzer and G. Gafner, *Acta Crystallogr.*, Sect. B., **26**, 985 (1970); S. Koda, A. Takenaka, and T. Watanabe, *Bull. Chem. Soc. Jpn*, **44**, 653 (1971).
(15) D. N. J. White and J. D. Dunitz, *Isr. J. Chem.*, **10**, 249 (1972).
(16) J. D. Dunitz and F. K. Winkler, *Acta Crystallogr.*, Sect. B, **31**, 251 (1975).
(17) K. Kraft and G. Koltzenburg, *Tetrahedron Lett.*, 4357 (1967).
(18) J. D. Dunitz and J. Waser, *J. Am. Chem. Soc.*, **94**, 5645 (1972).
(19) J. E. Kilpatrick, K. S. Pitzer, and R. Spitzer, *J. Am. Chem. Soc.*, **69**, 2483 (1947).
(20) We have recently described a pseudorotational degree of freedom as corresponding to a one-dimensional partial inflection point with zero slope.[3] This definition is, however, incomplete: The conditions for such an inflection point are necessary, yet not sufficient conditions for a pseudorotational degree of freedom.

Conformations of Glycyl-*trans*-4-fluoro-L-prolyl-L-tryptophan in Aqueous Solution[1]

J. T. Gerig* and R. S. McLeod

Contribution from the Department of Chemistry, University of California, Santa Barbara, California 93106. *Received August 26, 1975*

Abstract: High-resolution proton and fluorine magnetic resonance spectra of the title tripeptide have been analyzed. Two conformational forms are indicated by the data; these most likely arise from restricted rotation about the glycyl-4-fluoroprolyl peptide bond. Consideration of the vicinal coupling constants suggests that the proline ring in each isomer is in an envelope conformation with C_δ the puckered atom.

Proline (I) is the only common cyclic α-imino acid found in globular proteins, and its appearance in the amino acid sequence of a protein often signals an abrupt change in tertiary structure.[2] Because of this the conformational attributes of the pyrrolidine ring in proline and proline-containing peptides have been of continuing interest. Of the techniques that have been applied in the study of this ring system, x-ray and neutron diffraction have probably been most revealing, and these studies have shown that in linear peptides with proline as a central residue, C_γ is the most mobile, appearing above or